HUNGARIAN JOURNAL OF
INDUSTRY AND CHEMISTRY
Vol. 54(2) pp. 87–94 (2026)
hjic.mk.uni-pannon.hu
DOI: 10.33927/hjic-2026-31

HUNGARIAN JOURNAL OF INDUSTRY AND CHEMISTRY
HJIC

EFFECT OF PRINT ORIENTATION AND INFILL ON THE CHARPY IMPACT STRENGTH OF FDM-PRINTED ABS

GÁBOR KERÉNYI[1] AND BALÁZS MIKÓ[1]*

1 Institute of Mechanical Engineering and Technology, Óbuda University, József körút 8., Budapest, 1081, HUNGARY

The paper presents an experimental investigation of the impact strength of FDM-printed specimens. Charpy impact test specimens were prepared according to ISO 148 geometry. During the investigation, the impact energy of the test specimens was measured, the fracture surfaces were examined, and the obtained data were evaluated using analytical methods. Following the evaluation, the optimal orientation was determined, and, based on further measurements, the optimal infill associated with this orientation was identified. The article also contains data related to the reproducibility of the measurement and the relevant literature background. The results show that the F90 orientation (parallel to the Y axis) possesses the optimal energy absorption. Its average impact energy value is 0.76 J. Among specimens printed in the F90 orientation with different infill percentages, 30% infill resulted in the highest impact energy.

Keywords: additive technology, FDM printing, ABS material, charpy impact test

1. Introduction

Fused Deposition Modelling (FDM) is a widely used additive manufacturing technology. In recent years, it has been regarded as one of the most dynamically developing processes, fundamentally changing rapid prototyping and custom manufacturing. During production, FDM generates less material waste than subtractive manufacturing processes, making it more environmentally friendly than the manufacture of parts and prototypes by material removal.

FDM printing is a form of additive manufacturing (AM—additive manufacturing) based on the MEX (material extrusion) process. Extrusion is defined as an additive manufacturing process in which material is selectively dispensed through a nozzle. By means of MEX processes, many plastics can be extruded, but without exception, they must belong to the family of thermoplastic polymers [1].

The quality of the produced parts is influenced by many parameters, such as the temperature and quality of the bed, the nozzle diameter, layer thickness, material characteristics, cooling conditions, and the fan speed [2],[3].

Due to the widespread use of 3D printing, the actual quality of printed parts needs to be verified through mechanical testing [4,5,6]. Many studies have investigated tensile specimens, whereas far fewer have examined the Charpy impact test [7].

When printed parts are incorporated into structures, it is important that the resistance of the component to dynamic loading is known. The printing orientation greatly influences the resulting mechanical properties.

In the present article, the mechanical properties of Charpy test specimens printed using FDM technology are analyzed. The aim of the experiment is to examine the impact strength of specimens printed with Hilbert curve-based infill as a function of print orientation and infill percentage. During the investigations, ABS (acrylonitrile butadiene styrene) filament was used due to its high impact resistance and resistance to weathering, as well as its prominent role in industry. ABS is considered one of the most widely used engineering plastics, both in industrial and hobby applications.

2. Methods

During the Charpy impact test, the impact toughness of the material is evaluated. During the test, the Charpy pendulum breaks the specimen with a hammer and continues to swing. The absorbed energy is determined from the pendulum swing angle.

Several standards exist for performing the test, depending on the material class being examined. The ISO 148 European standard describes standardized testing of metals, while ASTM-E23 serves as the equivalent standard in the United States (USA). The

Received: 12 Apr 2026; Revised: 28 May 2026;
Accepted: 2 June 2026
*Correspondence: miko.balazs@bgk.uni-obuda.hu

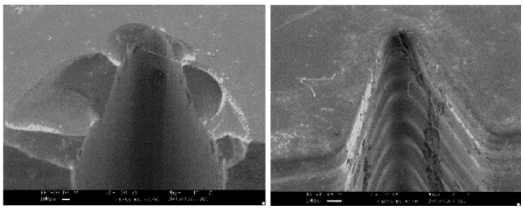


Figure 1: Mechanically and printed V-shaped notch [9]

geometric specifications are identical in both standards. For plastics, the applicable standards are ISO 179-1 (non-instrumented), ISO 179-2 (instrumented), and ASTM D6110. All three standards prescribe identical geometric parameters; however, these standards apply not to printed specimens but to extruded and injection-molded specimens.

Currently, no Charpy test-specific standard is included among the ASTM standards for additive manufacturing. Even in the 2015 publication (NIST IR 8059) of the National Institute of Standards and Technology (NIST), ISO 179 is described for impact energy testing [8]. Due to the absence of a specific testing standard dedicated to 3D-printed parts, the experimental methodology was based on the principles of ISO 179-1 standard. However, a deviation was made regarding the specimen geometry, adapting the dimensions specified in the ISO 148-1 standard instead of the conventional ISO 179-1 requirements. This modification was necessary because the smaller thickness (4 mm) prescribed by the standard plastic testing would fail to adequately demonstrate the structural effects of variable infill patterns.

A V-notch created by material removal weakens the printed structure. Microcracks and delamination may occur between the layers, resulting in lower impact resistance and reduced energy absorption for the polymer. Consequently, machining after printing negatively affects the mechanical resistance of the component. *Figure 1* shows a scanning electron microscope (SEM) image of a mechanical (left) and a printed notch (right) [9]. According to this study, the V-notch was created by printing.

The fracture tests were performed using a standard-compliant RM 201-type Charpy pendulum (*Figure 2*). The hammer was set to 0.4 kpm, which corresponds to 39.23 Nm. The support span was adjusted to 40 mm. The humidity in the test room was 29%, and the temperature was 18.9 °C, measured with a TOO WS-200-W type weather station. The environmental conditions were identical before and after the fracture test.

The geometric dimensions of the Charpy test specimens are identical to those specified in ISO 148-1. According to the standard, specimens with a length of 55 mm and a cross-section of 10 × 10 mm were printed with a layer thickness of 0.2 mm, each containing a printed V-shaped notch. The geometry of the test specimen is shown in *Figure 3*.

ABS is an impact-resistant thermoplastic (heat-softening) polymer belonging to the family of engineering plastics. It is an amorphous polymer, which



Figure 2: RM 201 type Charpy pendulum

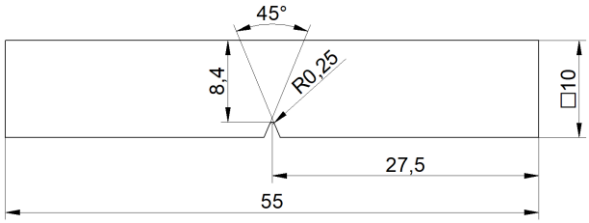


Figure 3: Specimen dimensions

is a terpolymer of polystyrene (PS) produced with butadiene and acrylonitrile [1],[3].

ABS is widely used. It can be utilized for injection moulding, blow moulding, and extrusion technologies. Its low melting point allows it to be used in additive manufacturing with FDM technology as well. Its extrusion temperature can be set between 230 and 270 °C. For printing, eSUN ABS+ 3D filament was used. The main properties of the raw material are included in *Table 1*.

Table 1: The material- and recommended printing parameters of ABS polymer

Parameter	Value
Density	1.04 g/cm^3
Melt flow index	12 (190 °C / 2.16 kg)
Tensile strength	43 MPa
Elongation	22 %
Flexural strength	66 MPa
Flexural modulus	1177 MPa
IZOD test	29 kJ/m^2
Deformation temperature	78 °C
Printing temperature	230-270 °C
Table temperature	95-110 °C
Printing speed	40-100 mm/s
Cooling fan speed	100 %

The infill pattern of the test specimens was designed based on a Hilbert curve. The Hilbert curve is a mathematically continuous, space-filling curve with a fractal structure. Fractal geometries are characterized by containing at least one mathematically describable repetition in their various forms. In fractal geometry, the concept of self-similarity is considered crucial. A Hilbert curve can be generated through mathematical iteration. Since a finite space is involved, it is referred to as a pseudo-Hilbert curve. Its order (number of iterations) determines the size and complexity of the infill. *Figure 4* illustrates the fifth order of the Hilbert curve. The infill pattern generated by Creality Slicer is shown in *Figure 5*.

The test specimens were produced using a Creality K1 FDM printer (*Figure 6*). The printer is equipped with an enclosed workspace, thereby reducing the influence of external temperature on print quality. The workspace measures 220 × 200 × 250 mm. It is equipped with a heated bed, which can be heated to 60 °C within 180 seconds, with a maximum temperature of 100 °C. High-speed printing is possible, with a feed rate of 600 mm/s, provided that the material is suitable for such speeds. This feature was not used during production.

The print head is equipped with dual fans, which ensure that the model solidifies before stringing or deformation occurs. The G-sensor in the print head measures the resonance frequencies during high-speed printing and automatically adjusts the printer to reduce

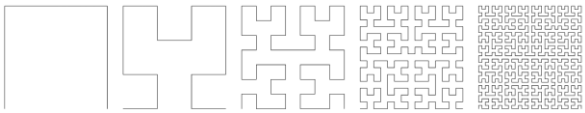


Figure 4: Increasing the order of the Hilbert curve



Figure 5: Infill pattern of the specimen



Figure 6: Creality K1 3D printer and Creality Space Pi Plus dryer

Table 2: Applied printing parameters

Parameter	Value
Speed	60 mm/s
Rapid speed	100 mm/s
Extruder temperature	260 °C
Bed temperature	100 °C
Chamber temperature	60 °C
Preheating temperature	65 °C
Layer thickness	0.2 mm
Nozzle diameter	0.4 mm
Number of shells	3
Infill structure	Hilbert-curve

related issues. The printable layer thickness ranges from 0.1 to 0.35 mm [10].

During printing, a Creality Space Pi Plus filament dryer and preheater were also used. With this device, the raw material can be heated to between 45–70 °C. Based on experience, printing ABS without drying results in bubbles in the printed parts due to moisture in the material. The dryer was set to 65 °C according to recommendations for ABS, and the device measured 13% humidity during printing. The raw material was fed to the printer through a tube, thereby protecting it from external influences [10]. The test specimens were produced with identical parameters, which are included in *Table 2*.

To investigate the effect of print orientation, four specimens were printed in the XY plane (marked as F), and four specimens were printed at an angle relative to the XY plane (marked as A). Three specimens were produced for each type.

The “F” specimens were rotated about the Z axis, and the number in their designation indicates the angle of rotation. The rotation was defined in the clockwise direction. The arrangement of the laid specimens is shown in *Figure 7*.

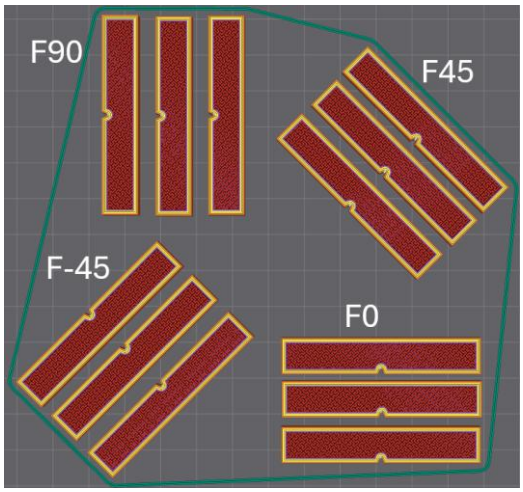


Figure 7: Horizontal orientation of the specimens

The "A" specimens were rotated in the YZ plane relative to the F90 orientation. The rotation angle is defined as the angle between the specimen and the XY plane. The arrangement of the tilted specimens can be seen in *Figure 8*. Support was required for printing, and an "organic tree" structure was used for this purpose. The support is indicated in green.

After the fracture tests of the F specimens, the most favorable orientation (F90) was further examined as a function of infill percentage. The different infill percentages are shown in *Figure 9*. The infill percentages were 50, 70, 90, and 99%. Considering both test phases (orientation and infill examination), a total of 36 specimens were produced.

3. Results

The results of the impact strength tests conducted to determine the ideal printing orientation are shown in *Figures 10 and 11*.

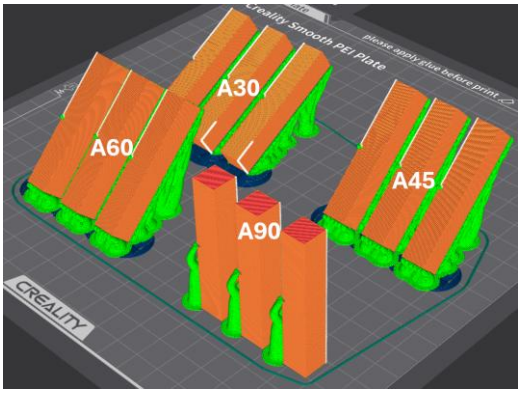


Figure 8: Inclined orientation of the specimens



Figure 9: Infill of F90 specimen

Unlike most studies that report results in kJ/m^2 as specific impact energy, the results are presented directly as absorbed impact energy in Joules [J]. This is because the partially filled Hilbert curve structure results in a non-homogeneous cross-section. Consequently, the actual load-bearing area cannot be determined explicitly, and conventional area-based normalization would distort the evaluation of material behavior.

Among the F specimens (printed in the XY plane), F-45 exhibited the lowest impact strength (0.53 J), while the specimen printed in the F90 orientation showed the highest energy absorption, with a value of 0.76 J. Among the tilted specimens, the highest impact energy was measured for A30 (0.58 J), and the lowest for A90 (0.06 J).

The standard deviations of the measured results are shown in *Figures 10 and 11*. The deviation from the average for the A45 specimens was minimal (0.0058 J), so this orientation exhibited the lowest measurement uncertainty. The highest standard deviation was observed for the F0 orientation, at 0.07 J.

To determine the infill percentage that provides the greatest resistance to mechanical loading, the data measured during the orientation examination served as the basis. During the investigation, the highest impact energy was achieved by the F90 specimen; therefore, additional specimens with different infill densities were printed in this orientation.

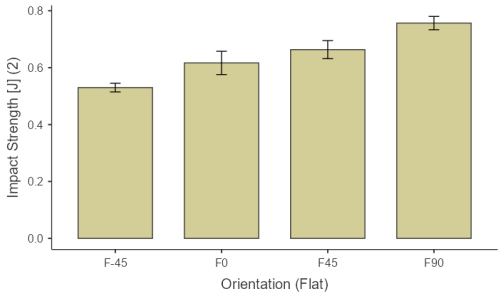


Figure 10: Impact strength of F series

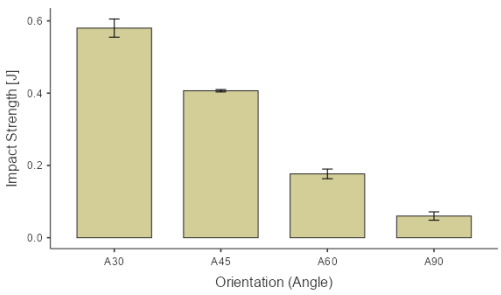


Figure 11: Impact strength of A series

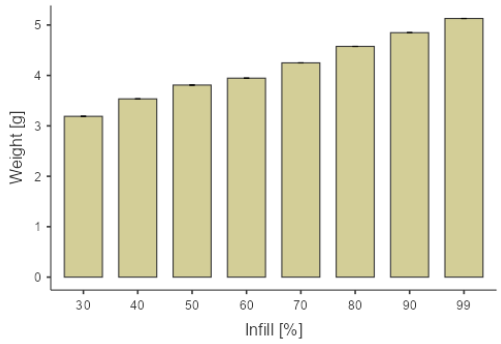


Figure 12: Weight of the specimens in function of infill rate

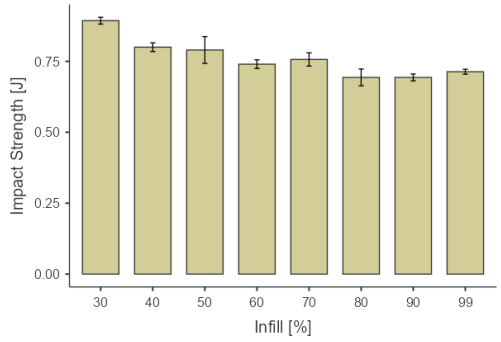


Figure 13: Impact strength in function of infill rate

To verify the accuracy of the infill, the mass of the specimens was measured (*Figure 12*). The measurement was performed with a Kern AIJ 220-4MN analytical balance. According to the diagram, the values increased in an approximately linear manner. The degree of deviation is negligible and, consequently, does not influence the measurement (0.0016–0.0068 g).

The highest standard deviation value was 0.08 J, which was observed for the specimen printed with 50% infill. Among the additional specimens printed in the F90 orientation (*Figure 13*), the specimen with 30% infill absorbed the most kinetic energy during the test, with a value of 0.89 J.

4. Discussion

The results indicate that the “F” specimens (*Figure 10*), which were laid flat in the XY plane, showed greater impact energy than the tilted specimens (*Figure 11*). The F90 orientation exhibited an average absorbed energy of 0.76 J. An exception is represented by the data for the F-45 and A30 specimens. The difference between the values was 0.05 J, so the two orientations can be considered nearly identical. However, it should be noted that the F-45 specimen has lower uncertainty.

The 45° raster angle investigated in the study by Ali et al. mechanically corresponds to the F90 orientation examined in this work. In perfect agreement with our findings, Ali et al. also identified this specific configuration as the optimal choice for maximizing impact properties [11]. Furthermore, a consistent conclusion was reached by Ahmad and Yahya, who similarly confirmed the superiority of this structural alignment in terms of energy absorption [12].

The print orientation with the highest energy absorption was F90. The average impact energy of F90 was 0.76 J. In this case, the direction of the fracture force was perpendicular to the layer orientation, resulting in higher resistance than that of the other specimens.

When examining the average values of F0, F45, and F90 separately, a linear trend can be observed. This can be explained by the fact that, in the case of these three specimens, their in-plane rotation was in the same direction, while for the F-45 specimen, it was in the opposite direction. This suggests that clockwise rotation had a positive effect on the changes in mechanical parameters in this case.

The lowest impact energy was measured for the A90 specimen, with an average value of 0.06 J. This can be explained by the fact that, in this case, only the strength of the adhesive bond could be measured in its entirety, as the direction of the force applied for fracture and the orientation of the layers were parallel to each other.

This structural vulnerability aligns with the findings of Kolekar et al., who reported that when the impact force is collinear with the layer interfaces, fracture toughness drops to its minimum due to rapid interlaminar shear and delamination [13].

Based on the measured data, the smaller the angle between the fracture force and the layer orientation, the lower the impact energy and, consequently, the energy absorption. Examining the “A” specimens, the impact energy values also display an almost linear behaviour as a function of the angle enclosed with the bed.

Increasing the infill resulted in denser and structurally more complex specimens. From this, it can be inferred that both the impact energy and the energy absorption capacity decrease with increasing infill, following a certain trend. As the infill increases, the internal structure loses flexibility, and, as a result, less energy can be absorbed and stored. Increasing the infill leads to more brittle fracture behavior.

Agrawal et al. demonstrated that increasing infill density enhances energy absorption; however, their study was limited to the upper range (75–85%). While our results confirm this increasing trend within that specific narrow interval, our broader investigation across the 30–99% range revealed a preceding decreasing trend. Consequently, analyzing the full spectrum demonstrates that a lower infill density can paradoxically yield higher energy absorption due to increased structural elasticity [14].

Figure 14 shows that the highest standard deviation occurred at 60% infill. In *Figure 15*, the specific (mass-independent) values of the data are presented, i.e., the impact strength was divided by the mass (IS/W). In this way, three groups can be distinguished: an elastic, a transitional, and a brittle data group. In this context, 30%

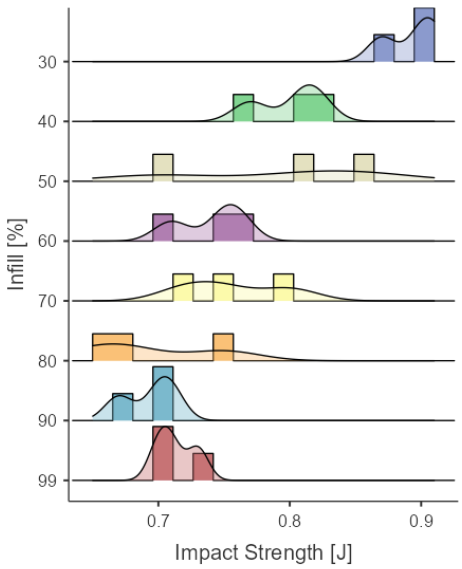


Figure 14: Density of the measured data

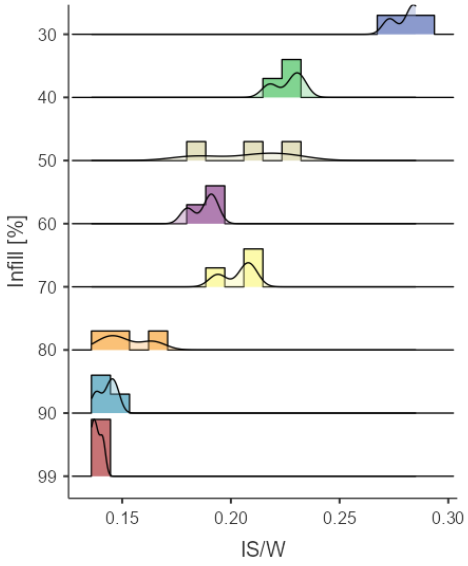


Figure 15: Density of the specific impact strength values

infill is considered elastic, 40–50–60–70% are transitional, and 80–90–99% infill can be regarded as brittle.

It can also be observed that the value of the impact energy increased and reached an upper limit at 80% infill, while in the brittle range, the standard deviation decreased, allowing printing with less uncertainty. Specimens with higher infill than this showed lower energy absorption.

Further examination of the F90 orientation showed that the lower the infill, the more energy can be absorbed by the internal structure.

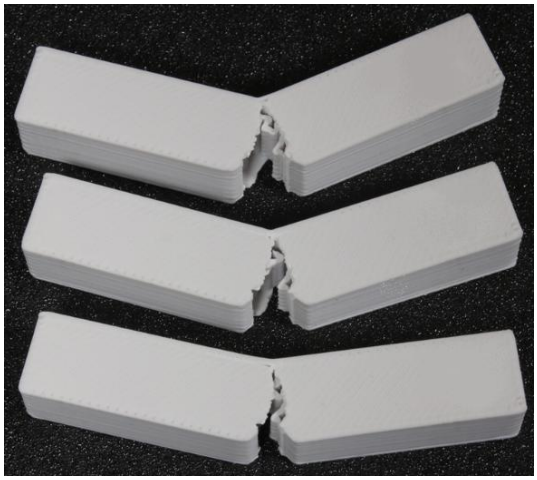


Figure 16: Fracture surface of the F90 70%



Figure 17: Fracture surface of the A90

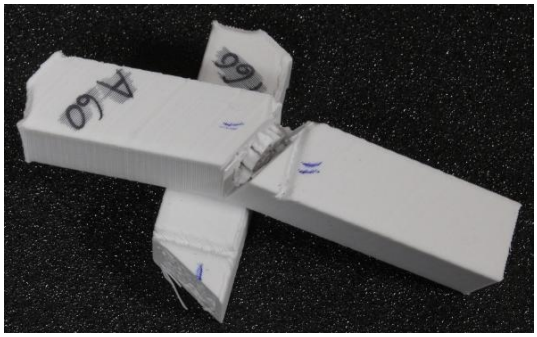


Figure 18: Fracture surface of the A60

During the orientation examination, the F90 specimen with 70% infill exhibited the highest impact energy. The fracture surface is shown in *Figure 16*.

From the fracture surface, it can be inferred that the printed specimen exhibits tough fracture characteristics. In cases where the fracture did not affect the entire cross-section, the wall of the structure appears to absorb most of the kinetic energy and hold the pieces together. In all such cases, the internal structure was torn out from the opposite side; thus, it had a limited contribution to energy absorption during impact.

In two cases, the fracture affected the entire cross-section: for the A90 (*Figure 17*) and A60 (*Figure 18*) specimens. In the case of A90, the specimens separated completely across their cross-sections. In one case, the

two sides remained attached; even then, however, only a single layer held the specimen together (*Figure 17*). These specimens suffered brittle fracture. As a result, their energy absorption was lower than that of the other specimens. Furthermore, the A60 specimen did not break along the notch. This can be explained by the fact that less force was required to break the adhesive bond than to cause fracture along the notch. The lowest impact energy was measured for A90 (*Figure 17*), with an average value of 0.06 J. This was due to the fact that, in this case, only the adhesive bond could be measured in its entirety, since the direction of the force applied for fracture and the orientation of the layers were parallel to each other.

In the infill examination, the F90 specimen with 30% infill exhibited the best energy absorption capacity, and its fracture surface is shown in *Figure 19*. Upon examining the surface, it was observed that, similar to the F90 specimen with 70% infill, the internal structure also broke out of the specimen. No delamination was observed. The outer shell remained intact. The fracture occurred entirely along the line of the applied force. Both the upper and lower shells were completely torn through. All three specimens produced the same fracture surface.



Figure 19: Fracture surface of the F90 30%

5. Summary

Additive manufacturing technology, and FDM in particular, is increasingly becoming part of engineering practice. From an application perspective, it is important to understand the strength properties of parts as a function of manufacturing parameters.

In this study, test specimens manufactured from ABS filament were examined using the Charpy test. The aim was to investigate the effect of print orientation and infill. Print orientation was investigated by placing the test specimens horizontally (F) and at an angle to the XY plane (A), and the infill was designed according to the Hilbert curve.

The F90 orientation resulted in the highest impact energy, with the load being perpendicular to the outer fibers in this case. The average impact energy of the specimen was 0.76 J.

The orientation was also examined with tilted specimens, where the angle enclosed with the bed was varied (A). It was observed that, in terms of impact energy, adhesion between the layers is the limiting factor. Increasing the infill does not improve performance if the direction of impact is perpendicular to the layer boundaries, as delamination occurs sooner than the material's own fracture. Such fractures occurred in the A90 and A60 specimens. Among the measured values, the lowest standard deviation was produced by the A45 specimen.

For the F90 orientation, Charpy specimens were produced with 30, 40, 50, 70, 80, 90, and 99% infill. With increasing infill, the impact energy and, consequently, the energy absorption capacity decreased. Within the examined range, 30% infill exhibited the highest impact energy, as well as the highest specific (mass-normalized) and absolute resistance. This can be explained by the fact that, at low infill, the lattice structure (infill pattern) can deform and bend, thereby absorbing energy before the entire cross-section fractures. In contrast, the 99% infill is more brittle, and cracks propagate more rapidly through the more homogeneous specimen.

In terms of standard deviation, the data revealed that the smallest uncertainty and the lowest standard deviation were observed at 99% infill.

According to the specific values, the specimens can be classified into three groups: elastic, transitional, and brittle. The 30% infill is considered elastic, 40–50–60–70% are transitional, and 80–90–99% infill is regarded as brittle. Consequently, higher infill provides greater predictability, whereas lower infill provides greater energy absorption. From a practical perspective, this means that for components subjected to dynamic loading, material savings (lower infill) can result not only in greater economy but also in more favorable mechanical behavior.

As a direction for future research, it would be worthwhile to investigate the effect of other infill patterns (e.g., gyroid) at the 30% infill level as well. Therefore, future research will implement a full-factorial design of experiments (DoE) to evaluate the complete matrix of infill densities and print orientations.

REFERENCES

[1] Bhatia, A., & Sehgal, A. K. (2023). Additive manufacturing materials, methods and applications: A review. *Materials Today: Proceedings*, *81*(2), 1060–1067. https://doi.org/10.1016/j.matpr.2021.04.379

[2] Tzotzis, A., Manavis, A., Efkolidis, N., Garcia-Hernández, C., & Kyratsis, P. (2024). Analysis of the influence of structural characteristics on the tensile properties of fused filament fabricated ABS polymer using central composite design. *Applied Mechanics*, *5*(1), 20–35. https://doi.org/10.3390/applmech5010002

[3] Jaya Christiyan, K. G, Chandrasekhar, U., & Venkateswarlu, K. (2016). A study on the influence of process parameters on the Mechanical Properties of 3D printed ABS composite. *IOP Conference Series: Materials Science and Engineering, 114*, Article 012109. https://doi.org/10.1088/1757-899X/114/1/012109

[4] Drégelyi-Kiss Á. (2024). Application of experimental design-based predictive models and optimization in additive manufacturing – a review. *Hungarian Journal of Industry and Chemistry*, *52*(1), 55–70. https://doi.org/10.33927/hjic-2024-08

[5] Özsoy, K., Erçetin, A., & Çevik, Z. A. (2021). Comparison of mechanical properties of PLA and ABS based structures produced by fused deposition modelling additive manufacturing. *Avrupa Bilim Ve Teknoloji Dergisi*, *27*, 802–809. https://doi.org/10.31590/ejosat.983317

[6] Ropovik, R., Peti, D., & Hatala, M. (2025). Strength analyses of FDM products from additively strengthened PLA materials. *MM Science Journal*, *2025-September*, 8512–8519. https://doi.org/10.17973/MMSJ.2025_09_2025085

[7] Bolat, C., & Ergene, B. (2023). An experimental effort on impact properties of polylactic acid samples manufactured by additive manufacturing. *Duzce University Journal of Science and Technology*, *11*(2), 998–1013. https://doi.org/10.29130/dubited.1075259

[8] Forster, A. M. (2015). *Materials testing standards for additive manufacturing of polymer materials: State of the art and standards applicability* (NISTIR 8059). National Institute of Standards and Technology. https://doi.org/10.6028/NIST.IR.8059

[9] Dizon, J. R. C., Espera Jr., A. H., Chen, Q., & Advincula, R. C. (2018). Mechanical characterization of 3D-printed polymers. *Additive Manufacturing*, *20*, 44–67. https://doi.org/10.1016/j.addma.2017.12.002

[10] Creality Co., Ltd. (n.d.). *Creality official website*. http://www.creality.com/

[11] Ali, M. U., Nadeem, A., Ashfaq, B., Ullah, S., Waseem, M., Aslam, M. A., & Alam, Q. A. (2024). Optimizing impact toughness in 3D-printed PLA structures using Hilbert curve and honeycomb infill patterns. *Engineering Proceedings*, *75*(1), Article 27. https://doi.org/10.3390/engproc2024075027

[12] Ahmad, M. N., & Yahya, A. (2023). Effects of 3D printing parameters on mechanical properties of ABS samples. *Designs*, *7*(6), Article 136. https://doi.org/10.3390/designs7060136

[13] Kolekar, A.B., Bhosale, S.M., Salunkhe, M.S., & Raut, N. P. (2024). Effect of process parameters on impact strength and hardness of FDM printed ABS parts. *International Journal of Materials and Product Technology*, *68*(1/2), 107–123. https://doi.org/10.1504/IJMPT.2024.10061462

[14] Agrawal, A.P., Kumar, V., Kumar, J., Paramasivam, P., Dhanasekarand, S., & Prasad, L. (2023). An investigation of combined effect of infill pattern, density, and layer thickness on mechanical properties of 3D printed ABS by fused filament fabrication. *Heliyon*, *9*(6), Article e16531. https://doi.org/10.1016/j.heliyon.2023.e16531